Available online at www.sciencedirect.com
SCIENCE DIRECT®
Journal of Organometallic Chemistry 664 (2002) 188–200
Journal of Organometallic Chemistry
www.elsevier.com/locate/jorganchem

Preparation and structural characterization of six new diorganotin(IV) complexes of the $R_2Sn(SaleanH_2)$ and $R_2Sn(SalceanH_2)$ type (R = Me, ^{n}Bu, Ph)

Reyes García-Zarracino, Jesús Ramos-Quiñones, Herbert Höpfl *

Centro de Investigaciones Químicas, Universidad Autónoma del Estado de Morelos, Av. Universidad 1001, C.P. 62210 Cuernavaca, Mexico

Received 13 August 2002; received in revised form 30 September 2002; accepted 2 October 2002

Abstract

Six new diorganotin(IV) complexes have been prepared from R_2SnO (R = Me, ^{n}Bu, Ph) and the Salan ligands $SaleanH_4$ ($SaleanH_4$ = *N*,*N*′-bis(*o*-hydroxybenzyl)-1,2-diaminoethane) and $SalceanH_4$ ($SalceanH_4$ = *N*,*N*′-bis(*o*-hydroxybenzyl)-1,2-diaminocyclohexane) in order to determine the preferred coordination mode of these ligands in dependence of their flexibility and basicity as well as the steric bulk of the organic groups attached to the tin(IV) atom. The present NMR spectroscopic and X-ray crystallographic study shows that the $SaleanH_2$ and $SalceanH_2$ ligands prefer a *fac*–*fac* configuration when coordinated to a diorganotin(IV) fragment, in which the nitrogen atoms are located *trans* to the organic groups. Depending on the steric bulk of the organic substituents, the conformation of the coordinated ligand can vary with respect to the orientation of the benzyloxy phenyl rings. In the solution state there may exist a rapid equilibrium between these possible conformations. For related $R_2Sn(Salen)$ complexes so far only structures with *trans* configurations have been reported, however, for $SalanH_2$ complexes with other metal ions both examples with *fac*–*fac* and *fac*–*mer* configurations are known. In the solid state structure of one of the complexes studied in here an interesting C–H···π intermolecular contact between a chloroform molecule and an aromatic ring has been detected.

Keywords: Salen and Salan complexes with tin(IV); *cis* and *trans* isomers; *fac*–*fac* and *fac*–*mer* configuration; C–H···π intermolecular contact; X-ray crystallography

1. Introduction

For a long time organotin(IV) complexes have received attention only with respect to structural features, since the coordination number and geometry of the diorganotin(IV) atom can be quite variable. Recently, however, it has been discovered that some of these complexes have cytotoxic activity making them interesting also from a biological point of view [1–16].

A review of the literature shows that only a small number of tin(IV) complexes with a N_2O_2 donor system is known. Thereby, the N_2O_2 donor atoms are provided mostly either by two bidentate NO ligands, e.g. picolinic acid [17,18] or 8-hydroxyquinoline [19–23], or by one tetradentate ONNO ligand, e.g. ethylenediamine-*N*,*N*′-diacetate (edda) [24] or the Salen class of ligands (Salen = *N*,*N*′-ethylenebis(salicylideneimine)) [25–33], which have been the most studied so far. The most common coordination number of diorganotin(IV) complexes with a NO or ONNO donor system is 6, corresponding to a distorted octahedral or a skew-trapezoidal bipyramidal geometry. In all cases mentioned above the Sn–C and Sn–O bonds are covalent, while the two N→Sn bonds are coordinate covalent. However, the formation of tetravalent complexes without the N→Sn bonds [34] as well as the enhancement of the coordination number to seven is also possible, if there is little steric bulk around the central tin atom, either through coordination of a solvent molecule or through an intermolecular D→Sn interaction [35].

An important aspect in the structural chemistry of complexes with a $SnC_2N_2O_2$ core is that the spatial distribution of the coordinating atoms can be variable, i.e. the organic groups can be in *cis* or *trans* orientation

* Corresponding author. Tel./fax: +52-777-329-7997
E-mail address: hhopfl@buzon.uaem.mx (H. Höpfl).

0022-328X/02/$ - see front matter
PII: S0022-328X(02)01986-1

[17–19,21,23]. The situation is even more complex in the case of complexes with the tetradentate ONNO ligands, where three coordination modes are possible, which may be classified as *mer–mer*, *fac–mer* and *fac–fac* (Scheme 1).

Specially for the tetradentate ONNO ligands so far little is known about the mutual interplay of the different factors responsible for the formation of a complex with a specific coordination environment, such as variation of basicity, rigidity, chelate size, delocalization of electron density and steric bulk of the different functional groups and ligands attached to the tin(IV) atom. Considering that most of the NO and ONNO ligands used formerly for the formation of diorganotin(IV) complexes are quite rigid (vide supra), we decided to prepare complexes with a more flexible ligand system, in order to investigate more deeply, which spatial distribution is preferred in these systems. The two ligands explored in this contribution with respect to their complexation capacity with Me_2Sn, $^nBu_2Sn$ and Ph_2Sn(IV) are reduced versions of the Salen class of ligands (Scheme 2). The $SaleanH_4$ ($SaleanH_4 = N,N'$-bis(*o*-hydroxybenzyl)-1,2-diaminoethane) and $SalceanH_4$ ($SalceanH_4 = N,N'$-bis(*o*-hydroxybenzyl)-1,2-diaminocyclohexane) ligands outlined in Scheme 2 belong to the Salan class of ligands, whose chemistry with main group elements is still relatively unexplored. Known examples include complexes of Al [36–45], Ga [45,46] and Sn(II) [47]. As far as we know complexes with Sn(IV) have not been reported until now.

A review of the Cambridge Structural Database [48] shows that Salen ligands generally induce the *trans*-configuration in complexes with a six-coordinate metal environment. As a consequence of the C=N bond hydrogenation, for the reduced analogue $SaleanH_4$ one expects increased N-basicity and greater flexibility, which may result also in a folded coordination mode, thus enabling one of the three different coordination types described in Scheme 1. In the case of $SalceanH_4$ the ligand flexibility is reduced somewhat, thus being also an interesting case for this type of analysis.

In the following the preparation and structural characterization of six new diorganotin(IV) complexes with the $SaleanH_4$ and $SalceanH_4$ ligands is described.

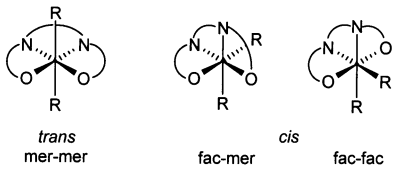

Scheme 1. Possible coordination modes of tetradentate ONNO ligands to a diorganotin(IV) moiety.

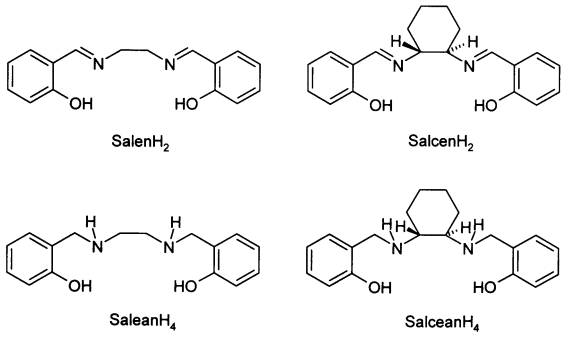

Scheme 2. $SaleanH_4$ and $SalceanH_4$ are the ligands used in this contribution for the formation of diorganotin(IV) complexes with a N_2O_2 donor system; their relationship to ligands of the Salen type is shown.

2. Results and discussion

2.1. Preparation of complexes 1–6

The $SaleanH_4$ and $SalceanH_4$ ligands have been prepared according to a literature procedure [49] by the reaction of two equivalents of salicyladehyde with 1,2-ethylenediamine and *trans*-1,2-cyclohexanediamine (racemic mixture), respectively, followed by reduction with $NaBH_4$ (Scheme 3). Complexes **1**–**3** have been obtained in yields of 42–57% by reaction of the tetradentate ONNO $SaleanH_4$ ligand with different diorganotin(IV) oxides R_2SnO (R = Me, ^{n}Bu, Ph) in a refluxing 5:1 solvent mixture of toluene and ethanol. Complexes **5**–**6** have been prepared in the same way with yields of 73–90% (Scheme 3), but compound **4** could be obtained in pure form only using the potassium salt $K_2[SalceanH_2]Cl_2$ and Me_2SnCl_2 (38% yield).

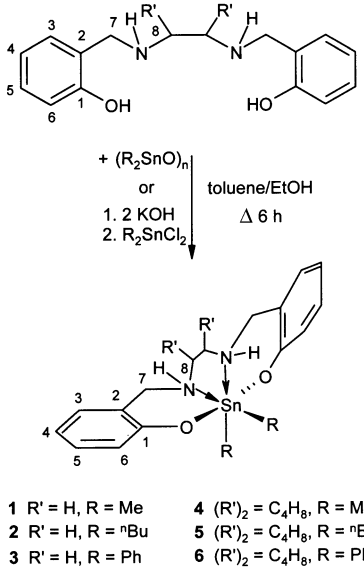

Scheme 3. Preparation of complexes **1**–**6**.

2.2. Spectroscopic characterization

For each of compounds **1**–**6** absorptions typical for the N–H vibrations were detected in the range 3225–3286 cm^{-1}, which are generally not significantly different from that of the ligands. The absorptions characteristic for the phenolic hydroxyl groups are missing, thus confirming the complexation of the ONNO ligands to the diorganotin(IV) moieties with formation of two covalent Sn–O bonds.

The ^{1}H- and ^{13}C-NMR spectra for **1**–**6** have been completely assigned using two-dimensional COSY, HETCOR, HMQC and COLOQ techniques. The most important chemical shifts have been summarized in Tables 1 and 2.

Analyzing the NMR data it is important to notice that there exists a significant chemical shift difference when benzene-d_6 is used as solvent instead of chloroform-d. This can be demonstrated for the case of the SaleanH$_4$ ligand and complex **1**, on comparing the shift displacements from the ^{1}H-NMR spectra recorded in $CDCl_3$ and C_6D_6 (Table 1). Interestingly, the most important shift differences result for the methylene hydrogen atoms PhCH_2N and NCH_2CH$_2$ with $\Delta\delta =$ 0.63–0.88 ppm for SaleanH$_4$ and $\Delta\delta = 0.65$–1.03 ppm for complex **1**. Therefore, in the following discussion of the ^{1}H-NMR data, compound **2** must be treated separately, since in this case the NMR data are available only in C_6D_6, while the spectra of the other five complexes have been recorded in $CDCl_3$.

As can be seen from Table 1 the ^{1}H-NMR data are indicative of a monomeric solution state geometry. Furthermore, in solution the complexes possess a mirror plane or a C_2-axis as symmetry element, since there are only signals for one molecule half in each case. Comparing SaleanH$_4$ and compounds **1**–**3**, the most important changes occur for the PhCH_2N and NCH_2CH$_2$ methylene groups, which appear as AB systems in each case, thus indicating that the chemical environments of the two hydrogen atoms within the two inequivalent methylene groups are different after complexation with the diorganotin(IV) fragment. The chemical shift differences for the AB systems are largest for the PhCH_2N hydrogens, $\Delta\delta = 1.00$ ppm for **1** in $CDCl_3$, $\Delta\delta = 1.28$ ppm for **1** in C_6D_6, $\Delta\delta = 1.29$ ppm for **2** in C_6D_6 and $\Delta\delta = 1.11$ ppm for **3** in $CDCl_3$. The corresponding shift differences for the NCH_2CH$_2$ hydrogens lie between $\Delta\delta = 0.09$ and 0.51 ppm. The NH groups are confirmed by the presence of broad signals at $\delta = 2.62$ ppm for **1** ($CDCl_3$), $\delta = 1.81$ ppm for **2** (C_6D_6) and $\delta =$ 2.65 ppm for **3** ($CDCl_3$). These observations prove N→Sn interactions with both nitrogen atoms.

The most relevant shift displacements in the ^{13}C-NMR spectra correspond to the carbon atoms bounded to the coordinating oxygen and nitrogen atoms. Thereby, the signals of the phenolic carbon atoms are shifted to lower fields by ca. 6.5 ppm, while the signals of the NCH_2CH$_2$ carbons move to higher fields by ca. 3 ppm. The signals corresponding to the PhCH_2N methylene carbon atoms apparently are almost not affected by the complexation.

The hexa-coordination of the tin(IV) core can be demonstrated also by ^{119}Sn-NMR spectroscopy, with signals at $\delta = -291$ ppm for **1**, $\delta = -336$ ppm for **2** and $\delta = -455$ ppm for **3**, being in the range of shift values reported for a series of hexa-coordinate diorganotin(IV) complexes with Salen derivatives [28,30,31]. For Me_2Sn-(oxin)$_2$ Bu_2Sn(oxin)$_2$ and Ph_2Sn(oxin)$_2$ (oxin = 8-hydroxyquinolinate) values of $\delta = -237$, -262 and -397 ppm have been reported [20], respectively, showing that SaleanH$_2$ provides higher electron density to the tin atom. The corresponding shift displacements of three R_2Sn(Salophen) complexes (Salophen = *N*,*N*′-1,2-phenylenebis(salicylideneimine)) are $\delta = -391$ (R = Me), -415 (R = ^{n}Bu) and -533 (R = Ph) ppm [30]. In the case of the Me_2Sn(IV) derivative the coordination number can be also deduced from the ^2J(Sn–H) coupling constant that has a value of 68 Hz [49]. From this coupling constant the C–Sn–C bond angle can be calculated: 118° [35]. The determination of the C–Sn–C bond angle from the ^1J(Sn–C) coupling constant gives values of 130° for **1** [50] and 141° for **2** [51].

The discussion of the ^{1}H-, ^{13}C- and ^{119}Sn-NMR spectra of SalceanH$_4$ and the corresponding complexes **4**–**6** is analogous, with the difference that now the NCH_2CH$_2$ methylene groups are substituted by a NC*H*R group due to the presence of the cyclohexyl moiety. AB systems are again observed for the PhCH_2N methylene hydrogens, not only for compounds **4**–**6**, but also for SalceanH$_4$ because of the chirality of the NC*H*R carbon atom. In comparison to **1**–**3**, the internal shift differences for the AB systems are lower, $\Delta\delta = 0.73$ ppm for **4**, $\Delta\delta = 0.72$ ppm for **5** and $\Delta\delta = 0.64$ ppm for **6**. With respect to the ^{13}C-NMR spectra the low field shifts for the phenolic carbon atoms and the high-field shift displacements of the NC*H*R carbons are both in the range of ca. 5 ppm. The ^{119}Sn-NMR spectra for **4**, **5** and **6** with signals at $\delta = -311$, -346 and -474 ppm, respectively, are slightly high-field shifted when compared with the ones measured for the Sn(SaleanH$_2$) analogues **1**–**3**. For **4** the C–Sn–C bond angle calculated from the ^2J(Sn–H) coupling constant is 118° [35], thus indicating that **1** and **4** have identical molecular configurations. However, from the ^1J(Sn–C) coupling constant C–Sn–C bond angles of 136 and 141° are predicted for **4** and **5**, respectively [50,51].

The mass spectral data of **1**–**6** indicate monomeric species in the gas phase. Although the molecular ion could be detected only for **1**, **2**, **3** and **6**, there is no doubt about the molecular structures of the other two com-

Table 1
Selected ^{1}H-NMR (400 MHz) spectroscopic data of SaleanH$_4$, SalceanH$_4$ and compounds **1**–**6** in $CDCl_3$ (ppm)

	NH	H3	H4	H5	H6	PhCH_2N	NCH_2CH$_2$	Hα/*o*-H	Hβ/*m*-H	Hγ/*p*-H	Hδ
SaleanH$_4$	–	6.97 (dd)	6.78 (dt)	7.19 (dt)	6.83 (dd)	4.00 (s)	2.85 (s)	–	–	–	–
SaleanH$_4$ [a]	–	7.14 (m)	6.79 (m)	7.14 (m)	6.79 (m)	3.37 (s)	1.97 (s)	–	–	–	–
1 (R = Me)	2.62 (s, br)	6.69 (d)	6.58 (t)	7.15 (dt)	6.91 (dd)	3.58, 4.58 (AB)	2.39, 2.48 (AB)	0.51 [b] (s)	–	–	–
1 (R = Me) [a]	1.36–1.87 (m)		6.65–7.15 (m)			2.65, 3.93 (AB)	1.36–1.87 (m)	0.57 [b] (s)	–	–	–
2 (R = Bu) [a]	1.81 (s, br)	6.66 (m)	6.66 (m)	7.22 (dt)	6.99 (d)	2.71, 4.00 (AB)	1.66 (m)	1.22 (m)	1.91 (m, br)	1.53 (h) [c]	1.01 (t)
3 (R = Ph)	2.65 (s, br)	6.86 (dd)	6.60 (dt)	7.24 (m)	7.01 (dd)	3.25, 4.36 (AB) [d]	2.26, 2.45 (AB)	8.09 [e] (dd)	7.35 (m)	7.30 (d)	–
SalceanH$_4$	–	6.98 (dd)	6.78 (ddd)	7.17 (ddd)	6.82 (dd)	3.93, 4.05 (AB)	2.45 (m)	–	–	–	–
4 (R = Me)	2.52 (br, s)	6.86 (d)	6.61 (ddd)	7.12 (t)	6.66 (dd)	3.93, 4.66 (AB)	2.62 (m)	0.46 [f] (s)	–	–	–
5 (R = Bu)	2.39 (m)	6.84 (dd)	6.58 (ddd)	7.11 (ddd)	6.64 (dd)	3.92, 4.64 (AB)	2.57 (m)	1.16 (m)	1.57 (m)	1.34 (m)	0.86 (m)
6 (R = Ph)	2.31 (d)	6.72 (dd)	6.59 (ddd)	7.21 (m)	6.97 (dd)	3.64, 4.28 (AB)	2.71 (m)	7.87 (dd) [g]	7.21 (m)	7.21 (m)	–

[a] Data in C_6D_6.
[b] ^2J(Sn–H) = 68 Hz.
[c] Hexuplett.
[d] ^3J(Sn–H) = 49 Hz.
[e] ^3J(Sn–H) = 70 Hz.
[f] ^2J(Sn–H) = 68 Hz.
[g] ^3J(Sn–H) = 71 Hz.

Table 2
Selected ^{13}C-NMR (100.5 MHz) spectroscopic data of SaleanH$_4$, SalceanH$_4$ and compounds **1**–**6** in $CDCl_3$ (ppm)

	C1	C2	C3	C4	C5	C6	C7	C8	Cα/*i*-C	Cβ/*o*-C	Cγ/*m*-C	Cδ/*p*-C
SaleanH$_4$	158.2	122.4	128.7	116.7	129.1	119.5	52.9	48.1	–	–	–	–
SaleanH$_4$ [a]	159.5	123.2	129.0 [b]	117.3	129.6 [b]	119.5	52.9	47.8	–	–	–	–
1 (R = Me) [a]	–	–	130.3 [b]	116.3	130.4 [b]	121.4	53.2	44.6	6.6 [c]	–	–	–
2 (R = Bu) [a,d]	165.7	121.7	130.4	116.2	130.5	121.3	53.5	45.0	25.4 [e]	29.3 [f]	28.1 [g]	14.5
3 (R = Ph)	164.7	122.0	130.4	116.7	130.5	120.6	53.4	45.3	150.0	136.3 [h]	28.5 [i]	128.7 [j]
SalceanH$_4$	158.2	123.2	128.5	116.7	129.1	119.4	50.0	60.1	–	–	–	–
4 (R = Me)	163.3	118.6	129.7	116.3	129.4	121.6	48.4	55.0	5.7 [k]	–	–	–
5 (R = Bu)	163.9	118.8	129.5	116.0	129.2	121.2	48.4	55.1	24.0 [l]	28.4 [m]	27.3 [n]	13.9
6 (R = Ph)	163.7	118.9	129.7	116.5	129.4	121.1	48.7	55.0	149.9	135.8 [o]	128.3 [p]	128.4

[a] Data in C_6D_6 as solvent.
[b] Data may be interchanged.
[c] ^1J(Sn–C) = 615 Hz.
[d] 50.3 MHz.
[e] ^1J(Sn–C) = 664 Hz.
[f] ^2J(Sn–C) = 21 Hz.
[g] ^3J(Sn–C) = 105 Hz.
[h] ^2J(Sn–C) = 47 Hz.
[i] ^3J(Sn–C) = 75 Hz.
[j] ^4J(Sn–C) = 16 Hz.
[k] ^1J(Sn–C) = 681 Hz.
[l] ^1J(Sn–C) = 658 Hz.
[m] ^2J(Sn–C) = 21 Hz.
[n] ^3J(Sn–C) = 109 Hz.
[o] ^2J(Sn–C) = 48 Hz.
[p] ^3J(Sn–C) = 78 Hz.

plexes, because the *m*/*z* mass ratios detected belong to ions formed through characteristic fragmentations.

2.3. Crystallographic study of *1*–*3* and *6*

The analysis of the spectroscopic data has demonstrated that the solution state structures of complexes **1**–**6** are monomeric and hexa-coordinate with a mirror plane or a C_2-axis as symmetry elements, thus corresponding either to a structure with a *trans*- or a *cis*–*fac*–*fac* configuration (Scheme 1). Please notice that the *cis*–*fac*–*mer* configuration possesses no symmetry element. For complexes with the Salen ligands, that have all resulted *trans*-isomers so far, two different conformations have been reported, one with a bow-shaped ligand conformation and mirror symmetry [30] and the other one with a stepped conformation and C_2-symmetry [27]. These configurations may be also proposed for the *trans*-isomer outlined in Scheme 1. Both for the *trans*-isomer and the *cis*–*fac*–*fac*-isomer, the hydrogen atoms within the PhCH_2N and NCH_2CH_2 methylene groups are in different chemical environments, so that these isomers are not distinguishable on hand of the NMR data available for **1**–**6**.

Therefore, in order to determine the correct configuration of the complexes studied in here, X-ray crystallographic studies have been realized for compounds **1**–**3** and **6**. The most relevant crystallographic data have been summarized in Table 3. Selected bond lengths, bond angles and torsion angles for **1**–**3** and **6** are outlined in Tables 4 and 5. The molecular structure for **1** is shown in Fig. 1. The asymmetric units of compounds **2** and **3** contain two independent molecules. While for **2** the molecular structures of the two independent molecules are practically identical (Fig. 2), for **3** the molecular geometries behave like pseudo-enantiomers (Fig. 3). Please notice that Fig. 3 does not represent the mutual orientation of the molecules in the asymmetric unit, on the contrary, the representation has been organized in such a way to show the above mentioned relationship. For compound **6** crystals with slightly different molecular structures could be grown from two different solvents, namely benzene and acetonitrile. A comparison of the two molecular structures is shown in Fig. 4.

In all four complexes the tin atoms are hexa-coordinated, having a distorted octahedral symmetry, with the organic alkyl or phenyl groups in *cis*-configuration and the tetradentate ONNO ligand coordinated in a *fac*–*fac* orientation. Molecular structures with SalanH$_2$ ligands bound to hexa-coordinated metal centers in the same fashion have been reported for molybdenum(VI) [53–55], tungsten(VI) [56,57], titanium(IV) [58] and zirconium(IV) [59] complexes. The *fac*–*mer* orientation was observed for some aluminium(III) [40,44], iron(III) [60–63] and chromium(III) [64,65] complexes.

The Sn–C bonds have lengths of 2.133(9)–2.168(4) Å that lie in the range expected for hexa-coordinated

Table 3
Crystallographic data for compounds **1**–**3** and **6** (CH_3CN and C_6H_6)

Compound	**1**	**2**	**3**	**6** (CH_3CN)	**6** (C_6H_6)
Formula	$C_{18}H_{24}N_2O_2Sn$, $CHCl_3$	$C_{24}H_{36}N_2O_2Sn$, 1.5 $CHCl_3$	$C_{28}H_{28}N_2O_2Sn$, 0.5 $CHCl_3$	$C_{32}H_{34}N_2O_2Sn$, 2 CH_3CN	$C_{32}H_{34}N_2O_2Sn$, C_6H_6
M	538.45	682.29	602.90	679.41	675.42
Crystal system	Triclinic	Triclinic	Orthorhombic	Monoclinic	Monoclinic
Space group	$P\bar{1}$	$P\bar{1}$	$P2_12_12_1$	$C2/c$	$C2/c$
a (Å)	7.8774(7)	11.251(2)	11.3722(6)	19.170(3)	19.1148(13)
b (Å)	11.4161(10)	13.974(3)	18.3910(10)	10.8226(16)	11.2387(8)
c (Å)	12.6450(11)	21.755(5)	25.7585(14)	18.137(3)	18.0168(12)
α (°)	82.8220(10)	77.001(3)	90	90	90
β (°)	85.8900(10)	89.658(4)	90	116.532(2)	121.1130(10)
γ (°)	79.354(2)	71.625(3)	90	90	90
U (Å^3)	1107.45(17)	3154.9(11)	5387.3(5)	3366.7(8)	3313.7(4)
Z	2	4	8	4	4
D_{calc} (Mg m^{-3})	1.615	1.436	1.487	1.340	1.354
μ (Mo–K$_\alpha$) (mm^{-1})	1.532	1.215	1.125	0.795	0.806
Crystal dimensions (mm)	0.24 × 0.10 × 0.06	0.48 × 0.46 × 0.27	0.33 × 0.24 × 0.19	0.30 × 0.19 × 0.06	0.38 × 0.08 × 0.08
Number of reflections measured	9024	36 583	52 354	15 937	15 682
Number of independent reflections	3410	14 480	9500	2965	2922
R_{int}	0.052	0.030	0.041	0.065	0.046
Number of observed reflections [a]	3113 [d]	11 111 [e]	9107 [e]	2606 [e]	2625 [e]
Number of variables	273	701	632	197	184
Goodness-of-fit	1.325	0.806	1.128	1.079	1.078
R [b]	0.0709	0.0494	0.0382	0.0436	0.0434
wR [c]	0.1516	0.1595	0.0959	0.0948	0.1171
$\Delta\rho_{max}$ (e Å^{-3})	1.405	1.102	0.882	0.522	1.170
$\Delta\rho_{min}$ (e Å^{-3})	−1.899	−0.568	−0.493	−0.988	−0.435

[a] $F_o > 4\sigma(F_o)$.
[b] $R = \Sigma(F_o^2 - F_c^2)/\Sigma\ F_o^2$.
[c] wR is for all data, $wR = [\Sigma\ w(F_o^2 - F_c^2)^2/\Sigma\ w(F_o^2)^2]^{1/2}$, $w^{-1} = \sigma^2 F_o^2 + (X \times P)^2 + 0.00P$; $P = (F_o^2 + 2F_c^2)/3$; $X = 0.0500$ for compound **1**, 0.1296 for compound **2**, 0.0571 for compound **3**, 0.0367 for compound **6** (CH_3CN) and 0.0601 for compound **6** (C_6H_6).
[d] θ Limits $2 < \theta < 24$.
[e] θ Limits $2 < \theta < 25$.

diorganotin(IV) complexes [17–19,21,22,24]. The Sn–O bonds with values between 2.073(3) and 2.155(3) Å are somewhat shorter than the corresponding bond lengths for a series of five R_2Sn(Salen) and R_2Sn(Salophen) complexes, 2.188(7)–2.237(2) Å [27,29–31]. In contrast, the N→Sn bonds are longer, 2.304(7)–2.431(4) Å for **1**–**3** and **6** ↔ 2.266(2)–2.290(9) Å for the above mentioned R_2Sn(Salen) derivatives. For the tetra-coordinated Sn(II)(Salen) complex Sn–O and Sn–N bond lengths of 2.007(3)–2.029(2) and 2.174(3)–2.191(3) Å, respectively, have been reported [32]. The N–Sn bonds in Me_2Sn(edda) are 2.346(3) Å long [24]. The lengthening of the N→Sn bonds comparing R_2Sn(Salen) with R_2Sn(Salan) derivatives can be explained by the change of hybridization of the nitrogen atom from sp^2 to sp^3, and does therefore, not necessarily contradict the above mentioned statement that a higher basicity is expected for the nitrogen atoms in the $SalanH_4$ type ligands.

For the four complexes under study the bond angles around the tin atom (Tables 4 and 5) show some variations according to the different steric bulk of the organic substituents at the tin atom, e.g. the O–Sn–O bond angles are increasing from 160.4(2)° for **1** to 164.9(2)–165.5(2)° for **2** and 165.1(2)–169.6(2)° for **3** and **6** on changing the R groups from Me to ^{n}Bu and Ph. Surprisingly, the C–Sn–C bond angles do not vary to the same extent, 106.1(4)° for **1**, 107.2(2)–107.5(3)° for **2** and 103.0(2)–107.5(2)° for **3** and **6**. As already discussed, for **1** the C–Sn–C bond angle can be calculated from the ^2J(Sn–H) and ^1J(Sn–C) coupling constants, with the observation that the better result is obtained from the calculation based on ^2J(Sn–H), 118↔130°. For **2** the ^2J(Sn–H) coupling constant could not be measured, and also in this case there is a large variation between the calculated C–Sn–C bond angle from ^1J(Sn–C), 141°, and the experimental one.

The distortion of the complexes from the ideal octahedral coordination geometry can be deduced from the already mentioned O–Sn–O and the *trans* C–Sn–N bond angles that are all significantly different from 180°: O–Sn–O = 160.4(2)–169.6(2)°, N–Sn–C = 159.2(2)–165.1(2)°. Accordingly, the bond angles in the

Table 4
Selected bond lengths (Å), bond angles (°) and torsion angles (°) for compounds **1**–**3**

	1	**2**	**3**
Bond lengths			
Sn1–O1	2.138(6)	2.152(3), 2.155(3)	2.083(4), 2.074(3)
Sn1–O2	2.095(6)	2.119(4), 2.124(4)	2.085(3), 2.074(3)
Sn1–N1	2.385(7)	2.406(4), 2.431(4)	2.356(4), 2.353(4)
Sn1–N2	2.304(7)	2.318(4), 2.327(4)	2.340(4), 2.349(4)
Sn1–C17	2.136(8)	2.153(6), 2.161(6)	2.153(5), 2.157(4)
Sn1–C18/C21/C23	2.133(9)	2.152(6), 2.174(6)	2.164(5), 2.160(5)
Bond angles			
O1–Sn1–O2	160.4(2)	165.5(2), 164.9(2)	166.82(15), 165.68(14)
O1–Sn1–N1	79.1(2)	79.3(1), 79.3(1)	82.53(14), 83.75(13)
O1–Sn1–C17	97.3(3)	97.7(2), 98.6(2)	96.6(2), 95.02(16)
O1–Sn1–C18/21/23	92.0(3)	90.7(2), 91.5(2)	91.82(18), 92.49(16)
O2–Sn1–N1	86.0(2)	87.7(2), 87.3(2)	87.23(15), 83.29(14)
O2–Sn1–C17	89.9(3)	89.2(2), 88.6(2)	91.76(19), 91.21(15)
O2–Sn1–C18/21/23	103.4(3)	99.6(2), 99.0(2)	96.06(19), 97.93(16)
N1–Sn1–C17	90.2(3)	92.3(2), 92.0(2)	90.50(18), 90.77(16)
N1–Sn1–C18/21/23	162.4(3)	159.2(2), 159.6(2)	165.12(17), 161.66(16)
N2–Sn1–C17	162.8(3)	162.7(2), 161.9(2)	163.39(18), 163.91(16)
O1–Sn1–N2	86.0(2)	88.0(1), 87.8(2)	86.10(16), 87.24(14)
O2–Sn1–N2	82.0(2)	81.9(2), 81.6(2)	83.05(15), 83.29(13)
N1–Sn1–N2	73.7(3)	72.5(2), 72.4(2)	73.54(17), 73.61(14)
N2–Sn1–C18/21/23	90.6(3)	89.0(2), 89.2(2)	92.40(17), 88.31(16)
C17–Sn1–C18/21/23	106.1(4)	107.2(2), 107.5(3)	103.86(19), 107.47(17)
Torsión angles			
Sn1–O1–C1–C2	−71.5(8)	−67.7(6), −67.6(5)	42.2(8), −35.8(7)
Sn1–O2–C12–C11	5.3(14)	32.1(8), 33.0(8)	46.7(6), −30.7(7)
O1–C1–C2–C7	−0.9(12)	−4.0(7), −5.1(7)	−1.2(9), −1.8(7)
O2–C12–C11–C10	−1.2(15)	−1.2(8), −2.0(8)	−1.5(7), −0.5(7)
C1–C2–C7–N1	61.0(11)	62.5(7), 63.7(7)	−57.6(7), 55.8(6)
C12–C11–C10–N2	44.0(13)	58.3(7), 59.1(7)	62.2(6), −53.2(6)
C2–C7–N1–Sn1	40.7(10)	42.0(6), 41.4(5)	−68.9(5), 64.4(5)
C11–C10–N2–Sn1	−68.7(9)	−74.1(5), −73.7(5)	−68.1(5), 67.7(5)
C7–N1–Sn1–O1	11.3(6)	9.1(4), 10.6(4)	30.5(3), −28.2(3
C10–N2–Sn1–O2	47.6(6)	37.7(3), 36.8(3)	26.0(3), −34.7(3)
N1–Sn1–O1–C1	63.9(5)	61.7(4), 62.6(4)	−21.5(5), 19.0(4)
N2–Sn1–O2–C12	16.1(8)	−11.1(5), −12.6(5)	−29.1(4), 10.7(4)
N1–C8–C9–N2	49.0(11)	50.4(6), 51.7(6)	46.1(7), −48.4(6)
C8–C9–N2–Sn1	24.4(10)	28.1(6), 29.5(6)	36.3(6), −35.3(5)
C9–N2–Sn1–N1	1.0(6)	−2.0(3), −3.1(3)	−14.1(3), 11.8(3)
N2–Sn1–N1–C8	26.6(6)	24.7(3), 23.9(3)	10.8(4), −13.8(3)
Sn1–N1–C8–C9	−48.1(9)	−47.6(5), −47.1(5)	−33.2(6), 37.3(5)

equatorial plane vary from 72.4(2) to 103.4(3)°. As expected, the N–Sn–N bond angles of the five-membered chelate rings are smaller than the O–Sn–N bond angles of the six-membered ones, 72.5(2)–73.6(2)↔ 79.1(2)–83.3(2)°.

The influence of the steric strain caused by the organic groups attached to the tin atom can be seen from the two different solid-state conformations of the SaleanH_4 complexes **1**–**3**. While the molecular structures of **1** and **2** are quite similar (Figs. 1 and 2), the molecular structure of **3** with the more voluminous phenyl groups (Fig. 3) has a different conformation, in which one of the phenyl rings of the benzyloxy moieties has been folded away from the organic substitutents. While the molecules in the solid state structure of **3** have a pseudo-

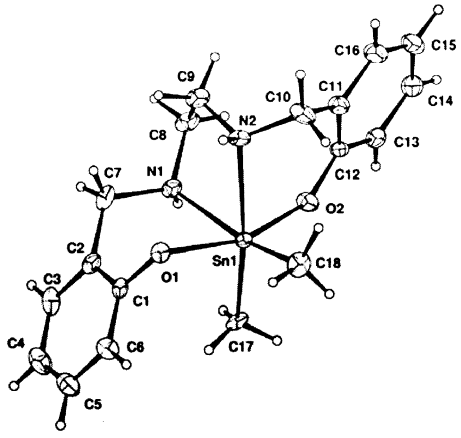

Fig. 1. Molecular structure of $Me_2Sn(SaleanH_2)$ (**1**).

Table 5
Selected bond lengths (Å), bond angles (°) and torsion angles (°) for compound **6** (crystallized from C_6H_6 and CH_3CN)

	6 (CH_3CN)	**6** (C_6H_6)
Bond lengths		
Sn1–O1	2.073(3)	2.076(3)
Sn1–N1	2.341(3)	2.343(3)
Sn1–C11	2.168(4)	2.167(4)
O1–C1	1.325(5)	1.338(5)
N1–C7	1.508(5)	1.492(6)
N1–C8	1.480(5)	1.498(5)
C2–C7	1.498(6)	1.498(7)
C8–C8′	1.514(7)	1.516(8)
Bond angles		
O1–Sn1–O1′	169.56(16)	165.12(17)
O1–Sn1–N1	79.68(11)	80.50(12)
O1–Sn1–C11	97.76(14)	96.76(14)
O1–Sn1–C11′	88.59(13)	92.50(14)
N1–Sn1–O1′	91.85(12)	87.49(13)
N1–Sn1–C11	92.15(13)	92.52(13)
N1–Sn1–C11′	160.20(13)	163.68(14)
N1–Sn1–N1′	72.53(15)	72.58(17)
C11–Sn1–C11′	105.3(2)	103.0(2)
O1–C1–C2	123.3(4)	124.5(4)
C1–C2–C7	121.6(4)	122.8(4)
N1–C7–C2	112.5(3)	112.9(4)
C7–N1–Sn1	110.4(2)	109.7(3)
C1–O1–Sn1	137.2(3)	133.8(3)
N1–C8–C8′	108.0(3)	107.4(3)
C8–N1–Sn1	112.8(2)	112.8(2)
Torsion angles		
Sn1–O1–C1–C2	10.0(7)	−4.9(6)
O1–C1–C2–C7	1.9(6)	6.4(7)
C1–C2–C7–N1	−46.8(5)	−44.8(6)
C2–C7–N1–Sn1	−70.9(4)	−69.9(4)
C7–N1–Sn1–O1	47.1(3)	51.9(3)
N1–Sn1–O1–C1	11.6(4)	24.1(4)
N1–C8–C8′–N1′	−56.4(7)	−57.4(7)
Sn1–N1–C8–C8′	43.3(4)	44.3(4)
C8′–N1′–Sn1–N1	−15.5(2)	−15.8(2)

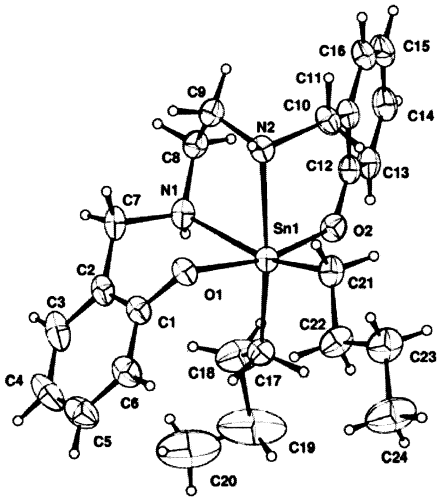

Fig. 2. Molecular structure of $^{n}Bu_2Sn(SaleanH_2)$ (**2**).

C_2 symmetry axis, the structures of **1** and **2** are completely asymmetric, which according to the NMR data permits the conclusion that in solution a rapid fluxional equilibrium between these two different conformations must exist. The molecular structures of the two modifications of compound **6** possess crystallographic C_2-symmetry, in which the folding of the benzyloxy phenyl groups is more flattened when compared with complex **3** (compare Figs. 3 and 4).

The structural differences between the two modifications of compound **6** indicate that there is some flexibility in adopting a specific molecular conformation (Table 5), which is probably influenced by intermolecular interactions in the crystal lattice. Thereby, it is important to notice that in both cases the solvent of crystallization forms part of the solid state structure, forming for the modification obtained from acetonitrile

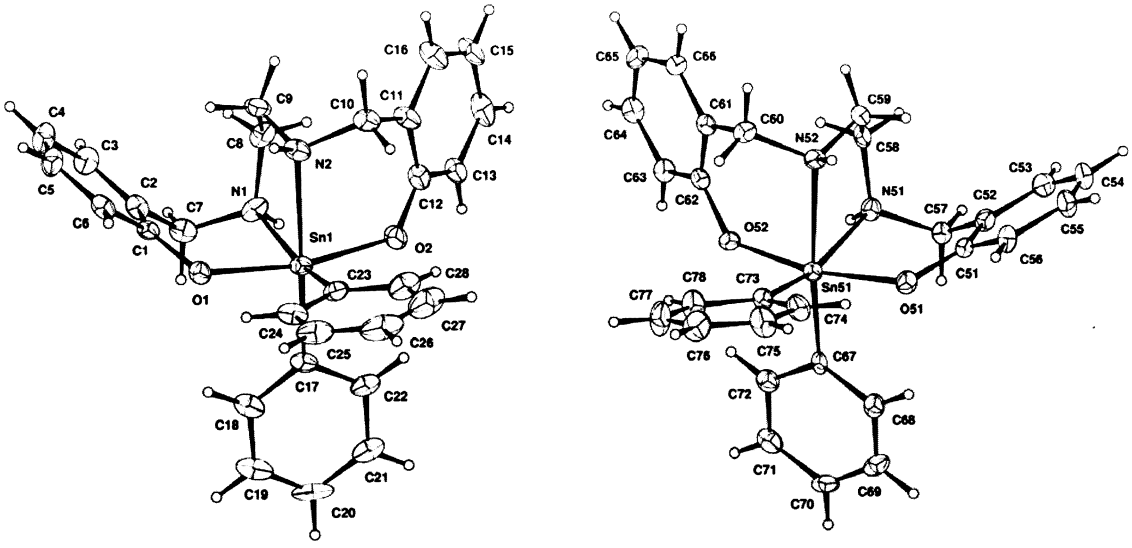

Fig. 3. The two independent molecules in the asymmetric unit of the crystal lattice of $Ph_2Sn(SaleanH_2)$ (**3**) are pseudo-enantiomers. Please notice that this figure does not represent the mutual orientation of the molecules in the asymmetric unit.

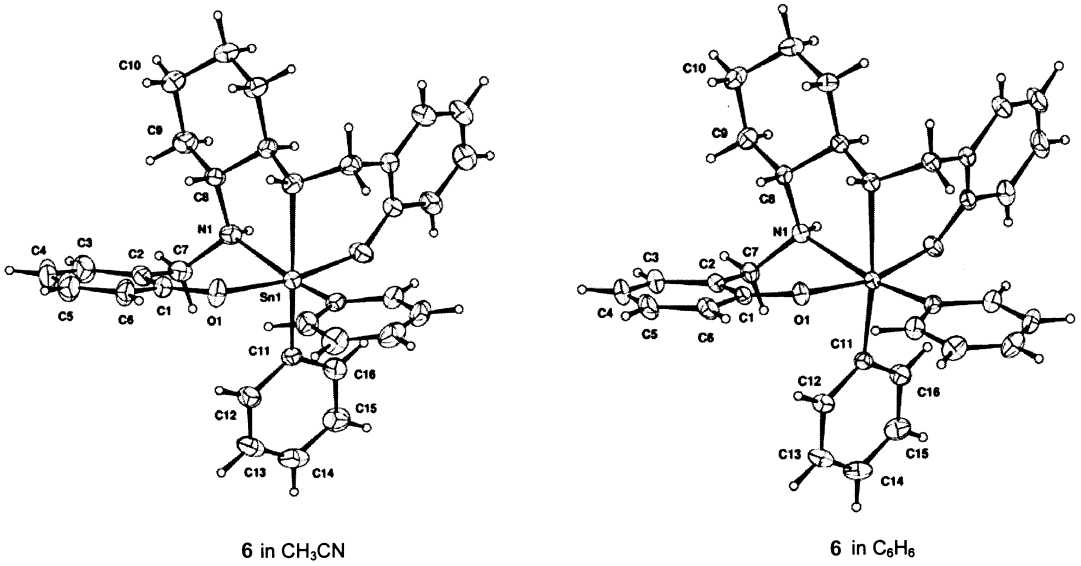

Fig. 4. Crystals of $Ph_2Sn(SalceanH_2)$ (**6**) could be grown from acetonitrile and benzene. The representation shows that the conformations of the molecular structures are slightly different.

an intermolecular N–H···N hydrogen bond between one of the amine hydrogens of the tin complex and the solvent molecule, 2.158 Å (3.043 Å, 164.2°). The crystal lattices of compounds **1**–**3** also contain different quantities of solvent molecules (chloroform) in their solid state structures, which participate in two different kinds of intermolecular interactions. For complex **1** there exist interesting C–H···π intermolecular contacts between the hydrogen atoms of the chloroform molecule and the centroids of one of the aromatic rings of the tin-complexes, 2.641 Å (3.607 Å, 168.8°). Recently, such interactions have received special attention [66]. For complex **2** intermolecular contacts between the chloroform molecules and the phenolic oxygen atoms are found, 2.252 (3.190 Å, 159.7°) and 2.220 Å (3.159 Å, 160.0°). Furthermore, in some cases there are intermolecular interactions between the tin complexes themselves, which have been summarized in Table 6.

3. Conclusions

The present study has shown that the $SaleanH_2$ and $SalceanH_2$ ligands prefer a *fac–fac* configuration when coordinated to a diorganotin(IV) fragment, in which the nitrogen atoms are located *trans* to the organic groups. Depending on the steric bulk of the organic substituents, the conformation of the coordinated ligand can vary with respect to the orientation of the benzyloxy phenyl rings. In the solution state probably there exists a rapid equilibrium between these possible conformations.

For related $R_2Sn(Salen)$ complexes so far only structures with *trans* configurations have been reported, however, for Salan complexes with other metal ions both examples with *fac–fac* and *fac–mer* configurations are known. Further studies are necessary in order to clarify, which factors direct the *cis*-isomers to the *fac–fac* or *fac–mer* coordination mode.

Table 6
Intermolecular contacts (Å, °) between the tin complex molecules in the crystal lattices of compounds **1**–**3**

Complex **1**	
N2–H···O1	1.976 (2.875, 169.2)
Complex **2**	
N2–H···O1	2.043 (2.950, 175.7)
N52–H···O51	2.058 (2.968, 177.5)
Complex **3**	
C26–H···O2	2.531 (3.440, 165.7)

4. Experimental

4.1. Instrumental

NMR studies were carried out on Varian Gemini 200 and Varian Inova 400 instruments. For ^{1}H- and ^{13}C-NMR $SiMe_4$ was used as internal standard and for ^{119}Sn-NMR $SnMe_4$ as external standard. Chemical shifts are stated in parts per million; they are positive, when the signal is shifted to higher frequencies than the standard. COSY, HETCOR, HMQC and COLOC experiments have been carried out in order to assign the ^{1}H and ^{13}C spectra completely. IR spectra have been recorded on a Bruker Vector 22 FT spectrophotometer. Mass spectra were obtained on a HP 5989 A equipment. Molecular weights for the analysis of the mass spectra were calculated using the most abundant tin isotope (^{120}Sn, 32.4%). For the realization of elemental analyses a Elementar Vario EL III equipment was used.

4.2. X-ray crystallography

X-ray diffraction studies of single crystals for compounds **1**–**3** and **6** were conducted on a BRUKER-AXS APEX diffractometer with a CCD area detector ($\lambda_{Mo-K_\alpha} = 0.71073$ Å, monochromator: graphite). A total of 2424 frames (complete sphere) was collected via ω-rotation ($\Delta/\omega = 0.3^\circ$) at 10 s per frame (program SMART [67]). For **2** only the hemisphere was collected at 5 s per frame due to decomposition of the crystals. The measured intensities were reduced to F^2 and corrected for absorption with SADABS (program SAINT-NT [68]), the cell parameters were determined by using reflections from all frames collected. Structure solution, refinement and data output were carried out with the SHELXTL-NT program package [69]. Non hydrogen atoms were refined anisotropically. Hydrogen atoms were placed in geometrically calculated positions using a riding model, however, in all cases the N–H hydrogen atoms have been located by difference Fourier maps. The molecular structures were created by the CRYSTALS software package [70,71].

All five crystal structures are characterized by the presence of solvent molecules in the crystal lattice, a different number of chloroform molecules in the case of compounds **1**–**3** and acetonitrile or benzene in the case of **6**. The asymmetric units of compounds **2** and **3** contain two independent molecules, which have practically the same configuration in the first case, but different ones in the second. The Sn–butyl groups in compound **2** are slightly disordered, therefore, restraints have been introduced. Crystals of compound **6** could be grown from two different solvents, benzene and acetonitrile, and have slightly different cell parameters due the inclusion of the solvent molecules in the crystal lattice. In both modifications the complex is located on a crystallographic C_2-axis, however, the molecular structures have slightly different configurations. The most important crystallographic data, selected bond lengths, bond angles and torsion angles have been summarized in Tables 3–5. The molecular structures are presented in Figs. 1–4.

4.3. Preparation of $SaleanH_4$ and $SalceanH_4$

Both ligands have been prepared according to a literature method [52]. Apparently, the spectroscopic data of $SalceanH_4$ have not been reported so far.

IR (KBr) ν_{max}: 3324 (w), 3298 (w), 2931 (m), 2853 (m), 2524 (m), 1591 (m), 1485 (m), 1456 (s), 1416 (m), 1368 (w), 1341 (w), 1263 (s), 1186 (w), 1153 (m), 1096 (m), 1020 (w).

^{1}H-NMR (400 MHz, $CDCl_3$) δ: 1.22 (m, 4H, H9, H10), 1.70 (m, 2H, H10′), 2.16 (m, 2H, H9′), 2.45 (m, 2H, H8), 3.93 and 4.05 (AB, 4H, H7), 6.78 (ddd, 2H, H4), 6.82 (dd, 2H, H6), 6.98 (dd, 2H, H3), 7.17 (ddd, 2H, H5) ppm. ^{13}C-NMR (100 MHz, $CDCl_3$) δ: 24.4 (C10), 30.7 (C9), 50.0 (C7), 60.1 (C8), 116.7 (C4), 119.4 (C6), 123.2 (C2), 128.5 (C3), 129.1 (C5), 158.2 (C1) ppm.

4.4. Preparation of $SaleanH_2Sn(IV)Me_2$ (**1**)

A solution of *N*,*N*′-bis(*o*-hydroxybenzyl)-1,2-diaminoethane (0.25 g, 0.92 mmol) and dimethyltin(IV) oxide (0.15 g, 0.92 mmol) in toluene–ethanol (5:1) is refluxed for 8 h using a Dean–Stark trap. After cooling down to room temperature (r.t.) the rest of the solvents is removed under vacuum obtaining a pale yellow product that was washed with hexane. Crystals suitable for X-ray crystallography were grown from chloroform. Yield: 57%. M.p. 190–194 °C.

IR (KBr) ν_{max}: 3286 (d), 3106 (m), 2994 (m), 2926 (m), 1595 (m), 1565 (m), 1480 (f), 1449 (f), 1298 (m), 1257 (m), 1218 (d), 1089 (d), 1028 (d), 952 (d), 882 (d), 854 (d), 751 (f), 575 (d), 512 (d) cm^{-1}.

MS (DIP) *m*/*z* (%): 418 [M, 5], 403 [M−Me, 100], 389 (15), 299 (33), 283 (63), 268 (10), 254 (23), 241 (18), 226 (16), 135 (16), 107 (73), 91 (19), 78 (38), 51 (11).

^{1}H-NMR (400 MHz, $CDCl_3$) δ: 0.51 (s, 6H, Hα, $^2J_{Sn-H} = 68$ Hz), 2.39 and 2.48 (AB, 4H, H8), 2.62 (s, br, 2H, NH), 3.58 and 4.58 (AB, 4H, H7), 6.58 (t, 2H, H4), 6.69 (d, 2H, H3), 6.91 (dd, 2H, H6), 7.15 (dt, 2H, H5) ppm. ^{1}H-NMR (200 MHz, C_6D_6) δ: 0.57 (s, 6H, Hα, $^2J_{Sn-H} = 68$ Hz), 1.36–1.87 (m, 6H, H8, NH), 2.65 and 3.93 (AB, 4H, H7), 6.65–7.15 (m, 8H, H3, H4, H5, H6) ppm. ^{13}C-NMR (50 MHz, C_6D_6) δ: 6.6 (Cα, $^1J_{Sn-C} = 615$ Hz), 44.6 (C8), 53.2 (C7), 116.3 (C4), 121.4 (C6), 130.3, 130.4 (C3, C5) ppm. ^{119}Sn-NMR (75 MHz, $CDCl_3$) δ: −291 (s) ppm.

Anal. Calc.: C, 51.56; H, 5.73; N, 6.68. Found: C, 53.82; H, 6.05; N, 7.08%.

4.5. Preparation of $SaleanH_2Sn(IV)^nBu_2$ (**2**)

A solution of *N*,*N*′-bis(*o*-hydroxybenzyl)-1,2-diaminoethane (0.25 g, 0.92 mmol) and di-*n*-butyltin(IV) oxide (0.18 g, 0.73 mmol) in toluene–ethanol (5:1) is refluxed for 8 h using a Dean–Stark trap. After cooling down to r.t. the rest of the solvents is removed under vacuum obtaining a pale yellow product that was washed with hexane. Crystals suitable for X-ray crystallography were grown from chloroform. Yield: 55%. M.p. 271–273 °C.

IR (KBr) ν_{max}: 3275 (d), 3124 (d), 3062 (d), 2953 (m), 2924 (m), 2864 (m), 1596 (m), 1568 (m), 1481 (f), 1452 (f), 1299 (f), 1266 (f), 1108 (d), 1074 (d), 1031 (d), 879 (m), 760 (m), 731 (d), 597 (d), 460 (d) cm^{-1}.

MS (DIP) *m*/*z* (%): 503 [M, 1], 446 [M−Bu, 24], 445 (43), 390 (10), 368 (12), 341 (99), 283 (45), 254 (44), 240 (34), 226 (62), 197 (11), 177 (41), 136 (37), 120 (29), 107 (100), 91 (49), 77 (39), 57 (49).

^{1}H-NMR (400 MHz, C_6D_6) δ: 1.01 (t, 6H, Hδ), 1.20 (m, 4H, Hα), 1.53 (hexuplett, 4H, Hγ), 1.66 (m, 4H, H8), 1.81 (s, br, 2H, NH), 1.91 (br, m, 4H, Hβ), 2.71 and 4.00 (AB, 4H, H7), 6.66 (m, 4H, H3, H4), 6.99 (d, 2H, H6), 7.22 (dt, 2H, H5) ppm. ^{13}C-NMR (100 MHz, C_6D_6) δ: 14.5 (Cδ), 25.4 (Cα, $^1J_{Sn-C} = 664$ Hz), 28.1 (Cβ, $^2J_{Sn-C} = 21$ Hz), 29.3 (Cγ, $^3J_{Sn-C} = 105$ Hz), 45.0 (C8), 53.5 (C7), 116.2 (C4), 121.3 (C6), 121.7 (C2), 130.4 (C3), 130.5 (C5), 165.7 (C1) ppm. ^{119}Sn-NMR (149 MHz, C_6D_6) δ: −336 (s) ppm. ^{119}Sn-NMR (149 MHz, $CDCl_3$) δ: −326 (s) ppm.

4.6. Preparation of SaleanH$_2$Sn(IV)Ph$_2$ (3)

A solution of *N*,*N*′-bis(*o*-hydroxybenzyl)-1,2-diaminoethane (0.24 g, 0.87 mmol) and diphenyltin(IV) oxide (0.25 g, 0.87 mmol) in toluene–ethanol (5:1) is refluxed for 8 h using a Dean–Stark trap. After cooling down to r.t. the rest of the solvents is removed under vacuum obtaining a colorless product that was washed with hexane. Crystals suitable for X-ray crystallography were grown from chloroform. Yield: 42%. M.p. 205–209 °C.

IR (KBr) ν_{max}: 3269 (d), 3257 (d), 3059 (d), 1597 (m), 1567 (m), 1480 (f), 1455 (f), 1472 (m), 1326 (m), 1294 (f), 1259 (m), 1070 (m), 1036 (m), 943 (d), 877 (m), 759 (m), 735 (m), 704 (m), 605 (d), 461 (d) cm^{-1}.

MS (DIP) *m*/*z* (%): 542 [M, 3], 465 [M−Ph, 41], 435 (6), 408 (46), 387 (32), 359 (21), 303 (38), 283 (76), 254 (30), 238 (15), 225 (25), 197 (65), 167 (22), 134 (15), 118 (21), 107 (100), 78 (64), 51 (24).

^{1}H-NMR (400 MHz, $CDCl_3$) δ: 2.26 and 2.45 (AB, 4H, H8), 2.65 (s, br, 2H, NH), 3.25 and 4.36 (AB, 4H, H7, $^3J_{Sn-H} = 49$ Hz), 6.60 (dt, 2H, H4), 6.86 (dd, 2H, H3), 7.01 (dd, 2H, H6), 7.24 (m, 2H, H5), 7.30 (d, 2H, *p*-H), 7.35 (m, 4H, *m*-H), 8.09 (dd, 4H, *o*-H, $^3J_{Sn-H} = 70$ Hz) ppm. ^{13}C-NMR (100 MHz, $CDCl_3$) δ: 45.3 (C8), 53.4 (C7), 116.7 (C4), 120.6 (C6), 122.0 (C2), 128.5 (*m*-C, $^3J_{Sn-C} = 75$ Hz), 128.7 (*p*-C, $^4J_{Sn-C} = 16$ Hz), 130.4 (C3), 130.5 (C5), 136.3 (*o*-C, $^2J_{Sn-C} = 47$ Hz), 150.0 (*i*-C), 164.7 (C1) ppm. ^{119}Sn-NMR (149 MHz, $CDCl_3$) δ: −455 (s) ppm.

Anal. Calc.: C, 56.82; H, 4.73; N, 4.65. Found: C, 57.22; H, 4.95; N, 4.69%.

4.7. Preparation of SalceanH$_2$Sn(IV)Me$_2$ (4)

The potassium salt of *N*,*N*′-bis(*o*-hydroxybenzyl)-1,2-diaminocyclohexane (0.58 g, 1.78 mmol) was prepared from a H_2O–EtOH solution containing 0.20 g (3.51 mmol) of potassium hydroxide. After addition of a solution of dimethyltin(IV)dichloride (0.38 g, 1.78 mmol) in H_2O a white precipitate formed, which was filtered and washed with small quantities of H_2O. Yield: 38%. M.p. 201–202 °C.

MS (DIP) *m*/*z* (%): 405 [M, 16], 299 (15), 283 (34), 270 (8), 254 (16), 241 (15), 226 (13), 173 (10), 149 (9), 136 (32), 120 (12), 107 (100), 91 (21), 77 (36), 51 (15).

^{1}H-NMR (400 MHz, $CDCl_3$) δ: 0.46 (s, 3H, Hα, $^2J_{Sn-H} = 68$ Hz), 0.95 (m, 2H, H10), 1.12 (m, 2H, H9), 1.71 (m, 2H, H9′), 2.52 (s, NH), 2.62 (m, 2H, H8), 2.80 (m, 2H, H10′), 3.93 and 4.66 (AB, 4H, H7), 6.61 (ddd, 2H, H4), 6.66 (dd, 2H, H6), 6.86 (d, 2H, H3), 7.12 (t, 2H, H5) ppm. ^{13}C-NMR (100 MHz, $CDCl_3$) δ: 5.7 (Cα, $^1J_{Sn-H} = 681$ Hz), 24.5 (C10), 29.5 (C9), 48.4 (C7), 55.0 (C8), 116.3 (C4), 118.6 (C2), 121.6 (C6), 129.4 (C5), 129.7 (C3), 163.3 (C1) ppm. ^{119}Sn-NMR (75 MHz, $CDCl_3$) δ: −311 (s) ppm.

Anal. Calc.: C, 55.85; H, 6.35; N, 5.92. Found: C, 54.70; H, 6.74; N, 5.53%.

4.8. Preparation of SalceanH$_2$Sn(IV)^{n}Bu$_2$ (5)

A solution of *N*,*N*′-bis(*o*-hydroxybenzyl)-1,2-diaminocyclohexane (0.25 g, 0.76 mmol) and di-*n*-butyltin(IV) oxide (0.19 g, 0.76 mmol) in toluene–ethanol (5:1) is refluxed for 8 h using a Dean–Stark trap. After cooling down to r.t. the rest of the solvents is removed under vacuum obtaining a pale yellow product that was washed with hexane. Yield: 90%. M.p. 207–209 °C.

IR (KBr) ν_{max}: 3225 (m), 2931 (m), 2855 (m), 1600 (m), 1563 (m), 1481 (f), 1451 (f), 1290 (f), 1267 (m), 1244 (m), 1102 (m), 1002 (d), 947 (d), 901 (m), 874 (m), 758 (m), 730 (m), 656 (m), 604 (m), 503 (m) cm^{-1}.

MS (DIP) *m*/*z* (%): 501 [M, 16], 395 (42), 337 (16), 240 (32), 229 (56), 122 (26), 107 (78), 96 (30) 91 (55), 77 (39), 57 (49), 41 (100).

^{1}H-NMR (400 MHz, $CDCl_3$) δ: 0.86 (m, 8H, Hδ, H9), 1.16 (m, 6H, Hα, H10), 1.34 (m, 4H, Hγ), 1.57 (m, 4H, Hβ), 1.69 (m, 2H, H10′), 2.27 (m, 2H, H9′), 2.39 (m, 2H, NH), 2.57 (m, 2H, H8), 3.92 and 4.64 (AB, 4H, H7), 6.58 (ddd, 2H, H4), 6.64 (dd, 2H, H6), 6.84 (dd, 2H, H3), 7.11 (ddd, 2H, H5) ppm. ^{13}C-NMR (100 MHz, $CDCl_3$) δ: 13.9 (Cδ), 24.0 (Cα, $^1J_{Sn-C} = 658$ Hz), 24.5 (C10), 27.3 (Cγ, $^3J_{Sn-C} = 109$ Hz), 28.4 (Cβ, $^2J_{Sn-C} = 21$ Hz), 29.4 (C9), 48.4 (C7), 55.1 (C8), 116.0 (C4), 118.8 (C2), 121.2 (C6), 129.2 (C5), 129.5 (C3), 163.9 (C1) ppm. ^{119}Sn-NMR (149 MHz, $CDCl_3$) δ: −346 (s) ppm.

Anal. Calc.: C, 60.36; H, 7.54; N, 5.03. Found: C, 59.16; H, 7.07; N, 4.95%.

4.9. Preparation of SalceanH$_2$Sn(IV)Ph$_2$ (6)

A solution of *N*,*N*′-bis(*o*-hydroxybenzyl)-1,2-diaminocyclohexane (0.25 g, 0.76 mmol) and diphenyltin(IV) oxide (0.22 g, 0.76 mmol) in toluene–ethanol (5:1) is refluxed for 8 h using a Dean–Stark trap. After cooling down to −20 °C a colorless product precipitates that was filtered. Crystals suitable for X-ray crystallography could be grown from benzene and acetonitrile. Yield: 73%. M.p. 181–183 °C.

IR (KBr) ν_{max}: 3245 (m), 3053 (m), 2934 (m), 2863 (m), 1597 (m), 1564 (m), 1482 (f), 1450 (f), 1288 (f), 1185 (d), 1149 (d), 1096 (m), 1068 (m), 1012 (m), 946 (d), 878 (m), 754 (m), 701 (m), 652 (d), 611 (m), 507 (m), 464 (m) cm^{-1}.

MS (DIP) *m/z* (%): 597 [M, 1], 521 (53), 443 (9), 415 (41), 351 (12), 337 (100), 303 (22), 229 (25), 197 (59), 120 (26), 107 (88), 91 (68), 77 (42), 56 (19), 51 (21). ^{1}H-NMR (400 MHz, $CDCl_3$) δ: 0.95 (m, 2H, H9), 1.11 (m, 2H, H10), 1.70 (m, 2H, H10′), 2.31 (m, 2H, H9′), 2.71 (m, 2H, H8), 3.64 and 4.28 (AB, 4H, H7), 6.59 (ddd, 2H, H4), 6.72 (dd, 2H, H3), 6.97 (dd, 2H, H6), 7.21 (m, 8H, H5, *m*-H, *p*-H), 7.87 (dd, 4H, *o*-H, $^{3}J_{Sn-H} = 71$ Hz) ppm. ^{13}C-NMR (100 MHz, $CDCl_3$) δ: 24.5 (C10), 29.6 (C9), 48.7 (C7), 55.0 (C8), 116.5 (C4), 118.9 (C2), 121.1 (C6), 128.3 (*m*-C, $^{3}J_{Sn-C} = 78$ Hz), 129.3 (*p*-C), 129.4 (C5), 129.7 (C3), 135.8 (*o*-C, $^{2}J_{Sn-C} = 48$ Hz), 149.9 (*i*-C), 163.7 (C1) ppm. ^{119}Sn-NMR (149 MHz, C_6D_6) δ: −474 (s) ppm.

5. Supplementary material

Crystallographic data for the structures reported in this paper have been deposited with the Cambridge Crystallographic Data Centre as supplementary publication numbers CCDC-191461–191465. Copies of the data can be obtained free of charge on application to The Director, CCDC, 12 Union Road, Cambridge CB2 1EZ, UK (Fax: +44-1223-336033; e-mail: deposit@ccdc.cam.ac.uk or www: http://www.ccdc.cam.ac.uk).

Acknowledgements

The authors thank CONACyT for financial support.

References

[1] A.J. Crowe, P.J. Smith, G. Atassi, Chem. Biol. Interact. 32 (1980) 171.
[2] A.J. Crowe, P.J. Smith, J. Organomet. Chem. 244 (1982) 223.
[3] A.J. Crowe, P.J. Smith, G. Atassi, Inorg. Chim. Acta 93 (1984) 179.
[4] A.J. Crowe, P.J. Smith, C.J. Cardin, H.E. Parge, F.E. Smith, Cancer Lett. 24 (1984) 45.
[5] F. Huber, G. Roge, L. Carl, G. Atassi, F. Spreafico, S. Filippeschi, R. Barbieri, A. Silvestri, E. Rivarola, G. Ruisi, F. Di Blanca, G. Alonzo, J. Chem. Soc. Dalton Trans. (1985) 523.
[6] A.J. Crowe, Drugs Future 12 (1987) 40.
[7] M. Gielen, C. Vanbellinghen, J. Gelan, R. Willem, Tetrahedron 45 (1989) 1219.
[8] N.M. Brown, Tin Based Antitumour Drugs, 1990, p. 69.
[9] R. Barbieri, A. Silvestri, J. Inorg. Biochem. 41 (1991) 31.
[10] R. Barbieri, Inorg. Chim. Acta 191 (1992) 253.
[11] M. Gielen, J. Meunier-Piret, M. Biesemans, R. Willem, A. El Khloufi, Appl. Organomet. Chem. 6 (1992) 57.
[12] M. Bouâlam, M. Biesemans, J. Meunier-Piret, R. Willem, M. Gielen, Appl. Organomet. Chem. 6 (1992) 197.
[13] M. Gielen, Metal Based Drugs 1 (1994) 213.
[14] M. Gielen, Coord. Chem. Rev. 151 (1996) 41.
[15] M. Nath, R. Yadav, M. Gielen, H. Dalil, D. Vos, G. Eng, Appl. Organomet. Chem. 11 (1997) 727.
[16] G.-D. Liu, J.-P. Liao, Y.-Z. Fang, S.-S. Huang, G.-L. Sheng, R.-Q. Yu, Anal. Sci. 18 (2002) 391.
[17] M. Gielen, M. Bouâlam, E.R.T. Tiekink, Main Group Met. Chem. 16 (1993) 251.
[18] K. Jurkschat, E.R.T. Tiekink, Main Group Met. Chem. 17 (1994) 659.
[19] E.O. Schlemper, Inorg. Chem. 6 (1967) 2012.
[20] J. Otera, J. Organomet. Chem. 221 (1981) 57.
[21] V.G.K. Das, C. Wei, Y.C. Keong, E. Sinn, J. Chem. Soc. Chem. Commun. (1984) 1418.
[22] D. Shi, Z.S. Hu, Jiegou Huexue 7 (1988) 111.
[23] A. Lycka, J. Holecek, M. Nádvorník, Main Group Met. Chem. 12 (1989) 169.
[24] S. Aizawa, T. Natsume, K. Hatano, S. Funahashi, Inorg. Chim. Acta 248 (1996) 215.
[25] A.V.D. Bergen, R.J. Cozens, K.S. Murray, J. Chem. Soc. A (1970) 3060.
[26] K. Kawakami, M. Miya-Uchi, T. Tanaka, J. Inorg. Nucl. Chem. 33 (1971) 3373.
[27] M. Calligaris, G. Nardin, L. Randaccio, J. Chem. Soc. Dalton Trans. (1972) 2003.
[28] A.M.V.D. Bergen, J.D. Cashion, G.D. Fallon, B.O. West, Aust. J. Chem. 43 (1990) 1559.
[29] S.-G. Teoh, G.-Y. Yeap, C.-C. Loh, L.-W. Foong, S.-B. Teo, H.-K. Fun, Polyhedron 16 (1997) 2213.
[30] D.K. Dey, M.K. Saha, M.K. Das, N. Bhartiya, R.K. Bansal, G. Rosair, S. Mitra, Polyhedron 18 (1999) 2687.
[31] D.K. Dey, M.K. Das, H. Nöth, Z. Naturforsch. Teil. B 54 (1999) 145.
[32] D. Agustin, G. Rima, H. Gornitzka, J. Barrau, J. Organomet. Chem. 592 (1999) 1.
[33] B. Yearwood, S. Parkin, D.A. Atwood, Inorg. Chim. Acta, 333 (2002) 124.
[34] M.S. Singh, K. Tawade, A.K. Singh, Main Group Met. Chem. 22 (1999) 175.
[35] T.P. Lockhart, F. Davidson, Organometallics 6 (1987) 2471.
[36] D.A. Atwood, J.A. Jegier, K.J. Martin, D. Rutherford, Organometallics 14 (1995) 1453.
[37] D.A. Atwood, D. Rutherford, Inorg. Chem. 34 (1995) 4008.
[38] D.A. Atwood, J.A. Jegier, D. Rutherford, J. Am. Chem. Soc. 117 (1995) 6779.
[39] D.A. Atwood, J.A. Jegier, M.P. Remington, D. Rutherford, Aust. J. Chem. 49 (1996) 1333.
[40] D.A. Atwood, J.A. Jegier, N.F. Lindholm, K.J. Martin, D. Rutherford, J. Coord. Chem. 38 (1996) 305.
[41] D.A. Atwood, J.A. Jegier, D. Rutherford, Inorg. Chem. 35 (1996) 63.
[42] D.A. Atwood, M.P. Remington, D. Rutherford, Organometallics 15 (1996) 4763.
[43] P. Wei, D.A. Atwood, Chem. Commun. (1997) 1427.
[44] P. Wei, D.A. Atwood, Polyhedron 18 (1999) 641.
[45] D.A. Atwood, D. Rutherford, Organometallics 14 (1995) 3988.
[46] D.A. Atwood, D. Rutherford, Organometallics 14 (1995) 2880.
[47] D.A. Atwood, J.A. Jegier, K.J. Martin, D. Rutherford, J. Organomet. Chem. 503 (1995) C4.
[48] Cambridge Structural Database, Cambridge Crystallographic Data Centre, Cambridge, UK, (April 2002).
[49] B. Wrackmeyer, Ann. Rep. NMR Spectrosc. 16 (1985) 73.
[50] T.P. Lockhart, W.F. Manders, J. Am. Chem. Soc. 109 (1987) 7015.

[51] J. Holecek, M. Nadvornik, K. Handlir, A. Lycka, J. Organomet. Chem. 315 (1986) 299.
[52] D.A. Atwood, J. Benson, J.A. Jegier, N.F. Lindholm, K.J. Martin, R.J. Pitura, D. Rutherford, Main Group Met. Chem. 1 (1995) 99.
[53] P. Subramanian, J.T. Spence, R. Ortega, J.H. Enemark, Inorg. Chem. 23 (1984) 2564.
[54] C.J. Hinshaw, G. Peng, R. Singh, J.T. Spence, J.H. Enemark, M. Bruck, J. Kristofzski, S.L. Merbs, R.B. Ortega, P.A. Wexler, Inorg. Chem. 28 (1989) 4483.
[55] H. Elias, F. Stock, C. Rohr, Acta Crystallogr. Sect. C 53 (1997) 862.
[56] Y.-L. Wong, Y. Yan, E.S.H. Chan, Q. Yang, T.C.W. Mak, D.K.P. Ng, J. Chem. Soc. Dalton Trans. (1998) 3057.
[57] Y.-L. Wong, J.-F. Ma, W.-F. Law, Y. Yan, W.-T Wong, Z.-Y. Zhang, T.C.W. Mak, D.K.P. Ng, Eur. J. Inorg. Chem. (1999) 313.
[58] J. Balsells, P.J. Carroll, P.J. Walsh, Inorg. Chem. 40 (2001) 5568.
[59] E.Y. Tshuva, I. Goldberg, M. Kol, J. Am. Chem. Soc. 122 (2000) 10706.
[60] L. Borer, L. Thalken, C. Ceccarelli, M. Glick, J.H. Zhang, W.M. Reiff, Inorg. Chem. 22 (1983) 1719.
[61] R. Viswanathan, M. Palaniandavar, P. Prabakaran, P.T. Muthiah, Inorg. Chem. 37 (1998) 3881.
[62] P. Mialane, E. Anxolabehere-Mallart, G. Blondin, A. Nivorojkine, J. Guilhem, L. Tchertanova, M. Cesario, N. Ravi, E. Bominaar, J.-J. Girerd, E. Munck, Inorg. Chim. Acta 263 (1997) 367.
[63] P. Baran, A. Bottcher, H. Elias, W. Haase, M. Huber, H. Fuess, H. Paulus, Z. Naturforsch. Teil. B 47 (1992) 1681.
[64] R. Sanzenbacher, A. Bottcher, H. Elias, M. Huber, W. Haase, J. Glerup, T.B. Jensen, M. Neuburger, M. Zehnder, J. Springborg, C.E. Olsen, Inorg. Chem. 35 (1996) 7493.
[65] A. Bottcher, H. Elias, J. Glerup, M. Neuburger, C.E. Olsen, H. Paulus, J. Springborg, M. Zehnder, Acta Chem. Scand. 48 (1994) 967.
[66] M.J. Calhorda, Chem. Commun. (2000) 801.
[67] Bruker Analytical X-ray Systems. SMART: Bruker Molecular Analysis Research Tool V. 5.618, 2000.
[68] Bruker Analytical X-ray Systems. SAINT+NT Version 6.04, 2001.
[69] Bruker Analytical X ray Systems. SHELXTL-NT Version 6.10, 2000.
[70] D.J. Watkin, C.K. Prout, J.R. Carruthers, P.W. Betteridge, T.I. Cooper, CRYSTALS, Issue 11, Chemical Crystallography Laboratory Oxford, Oxford, 2000.
[71] D.J. Watkin, C.K. Prout, L.J. Pearce, CAMERON, Chemical Crystallography Laboratory Oxford, Oxford, 1996.